First Direct Observation of Elementary Steps on the Surfaces of Glucose Isomerase Crystals under High Pressure

ARTICLE *in* CRYSTAL GROWTH & DESIGN · OCTOBER 2009

Impact Factor: 4.89 · DOI: 10.1021/cg800119w

6 AUTHORS, INCLUDING:

Yoshihisa Suzuki
The University of Tokushima
82 PUBLICATIONS **670** CITATIONS
SEE PROFILE

Gen Sazaki
Hokkaido University
166 PUBLICATIONS **2,440** CITATIONS
SEE PROFILE

DOI: 10.1021/cg800119w

CRYSTAL GROWTH & DESIGN Article

2009, Vol. 9
4289–4295

First Direct Observation of Elementary Steps on the Surfaces of Glucose Isomerase Crystals under High Pressure

Yoshihisa Suzuki,*[,#,†] Gen Sazaki,[#,‡,¶] Masamitsu Matsumoto,[§] Makoto Nagasawa,[§] Kazuo Nakajima,[‡] and Katsuhiro Tamura[†]

[†]*Department of Life System, Institute of Technology and Science, The University of Tokushima, 2-1 Minamijosanjima, Tokushima 770-8506, Japan,* [‡]*Institute for Materials Research, Tohoku University, 2-1-1 Katahira, Aoba-ku, Sendai 980-8577, Japan, and* [§]*Syn-corporation, Ltd., 204 D-Egg, 1 Jizoudani, Koudo, Kyotanabe, Kyoto 610-0332, Japan.* [#] *Equal contribution.* [¶] *Present address: Institute of Low Temperature Science, Hokkaido University, N19-W8, Kita-ku, Sapporo 060-0819, Japan.*

Received January 31, 2008; Revised Manuscript Received August 17, 2009

ABSTRACT: We have succeeded in the first direct observation under high pressure of the elementary steps (7.2 nm high) on {011} faces of glucose isomerase (GI) crystals, by using a laser confocal microscope combined with a differential interference contrast microscope (LCM-DIM) and a specially designed high-pressure vessel with a sapphire window of 1 mm thickness. The images of elementary steps taken under 50 MPa exhibited a sufficiently high contrast level for subsequent studies of crystal growth. By in situ observations, we directly confirmed that, irrespective of pressure, {011} faces of GI crystals grew by two-dimensional (2D) nucleation growth of the polynucleation type, and that pressure did not affect growth morphology. We measured the solubility of GI crystals under high pressure by observing in situ the growth and dissolution of elementary steps and ridges on the crystals. The resulting solubility curve exhibited much higher precision than those determined by interferometry, and revealed a significant decrease in solubility with increasing pressure. We also measured the 2D nucleation rates of 2D islands and the velocities of elementary steps under high pressure.

Introduction

Three-dimensional structures of more than 30 000 proteins have been determined so far, mainly by X-ray crystallography. However, the protein crystallization process remains an obstacle to structural determination. In fact, only about 30% of purified proteins become crystallized;[1] this rate has not increased significantly in the past 20 years.

To find the key to improving the protein crystallization success rate, we believe it is necessary to identify the factors that accelerate the nucleation and growth of protein crystals. One such factor is the high-pressure acceleration, first found by Visuri et al.,[2] of the nucleation and growth of glucose isomerase (GI) crystals. In our previous studies, we revealed that high pressure accelerates the crystallization of GI by decreasing solubility (increasing supersaturation).[3] We also found that high pressure also accelerates the growth rates of the crystal faces even at the same supersaturation: we found that the growth kinetics accelerated under high pressure.[4] By analyzing the supersaturation dependencies of the face growth rates, we concluded that high pressure accelerates two-dimensional (2D) nucleation rates through the decrease in surface free energy,[4] which holds the key to the promotion of three-dimensional (3D) nucleation of protein crystals.[5,6] However, these previous studies, relying on interferometry and ordinary optical microscopy, had problems that hindered our ability to obtain further insights into high-pressure effects.

We previously measured the solubility of GI crystals under high pressure, using a Michelson type two-beam interferometer (TBI).[3] However, the extent of the errors included in the solubility curves determined by TBI prevented further detailed analyses of the growth kinetics of GI crystals. Since in our previous study[3] TBI detects the concentration distribution around a crystal,[3,7−13] a significant amount of growth or dissolution of a crystal is necessary for the detection, causing large errors in the solubility curves. If individual elementary steps can be observed in situ under high pressure, one can significantly improve the precision of solubility curves.

As for the growth kinetics of GI crystals, we measured in situ growth rates of {101} faces, R_{101}, of GI crystals under high pressure using ordinary optical microscopy,[4] and analyzed R_{101} using a 2D nucleation growth model of the polynucleation type. Since R_{101} is proportional to $J_s^{1/3}V^{2/3}$ (J_s: 2D nucleation rate, V: step velocity),[14] the model analyses of R_{101} are indirect and prevent further detailed analysis. In situ observation of the steps enables us to directly and separately measure J_s and V, which are necessary to elucidate the causes of high-pressure acceleration of the nucleation and growth. Hence, direct observation of individual elementary steps plays a crucial role in studies of crystallization under high pressure.

Direct observations of individual elementary steps on protein crystal surfaces have been carried out mainly by atomic force microscopy (AFM).[15−17] However, AFM does not work under high pressure (>6 atm)[18] at the present stage. Besides, the scan of a cantilever would potentially affect the soft surfaces of protein crystals. Advanced optical microscopy is a promising alternative to directly and noninvasively observe individual elementary steps even under high pressure. Among various kinds of advanced optical microscopy, we adopted laser confocal optical microscopy combined with differential interference contrast microscopy (LCM-DIM), by which we have already succeeded in observing the elementary steps of GI crystals under atmospheric pressure.[4] The development of a high-pressure vessel with an optical window thin enough to suppress optical aberration will also play a crucial role in advanced optical microscopy.

*To whom correspondence should be addressed. E-mail: suzuki@chem.tokushima-u.ac.jp.

Published on Web 09/09/2009

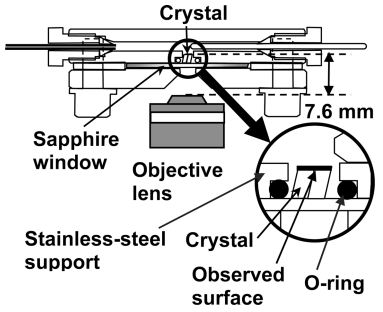

Figure 1. Schematic illustration of an experimental setup.

In this study, we utilized LCM-DIM and a newly developed high-pressure vessel with a thin sapphire window to attempt, for the first time, the direct observation of elementary steps of GI crystals under high pressure. In addition, utilizing this setup, we also tried the first preliminary studies on the solubility, J_s, and V of GI crystals under high pressure.

Experimental Section

Apparatus. This study made use of an LCM-DIM system (Olympus Optical Co., Ltd.) composed of a confocal unit FV300, an inverted optical microscope IX71, and a large shear length-type U-DICTHC Nomarski prism. The details of this system were explained in our previous studies.[6,19,20] With the previous system using a He−Ne laser as a light source, the appearance of interference fringes often diminished image quality. To eliminate the interference fringes, a superluminescent diode (SLD) laser (Amonics Ltd., model ASLD68-050-B-FA: λ = 680 nm), whose coherence length is about 10 μm, was adopted as a light source.

Figure 1 shows a schematic illustration of a high-pressure vessel and a GI crystal. A high-pressure vessel with a 1-mm-thick sapphire window (Syn-corporation, Ltd., PC-100-MS) was specially designed and used for the in situ observation of crystal surfaces under high pressure. We used an O-ring to provide a seal between the sapphire window and a stainless steel support. The surface of the support attached to the sapphire window was processed by mirror polishing to increase the pressure that the O-ring could withstand. In this study, achieving a balance in the thickness of the sapphire window was particularly important, since a thinner window decreases optical aberration, while a thicker one raises the withstand pressure. Although Abe et al.[21] used a thin and small (0.5 mm thick and 3.5 mmϕ) diamond window, this window would not have allowed our observation. We needed a larger (>8 mmϕ) single crystal to ensure an optical aperture size of 3 mmϕ, which is necessary for high-resolution observation utilizing the numerical aperture 0.55 and working distance 7.6 mm of the objective lens used in this study (Olympus Optical Co. Ltd., SLCPlanFl 40 ×); however, there are as yet no single synthetic diamonds larger than 8 mmϕ. To our knowledge, the vessel used in this study provides top performance in in situ observation of crystal surfaces. The volume of sample space in this vessel is 8.3 mm^3 (4.3 mm in height and 1.6 mm in diameter).

To compensate for the optical aberration caused by the light transmitted through the sapphire window, an objective with a compensation ring for a cover glass with a thickness of 0−2 mm (Olympus Optical Co., Ltd., SLCPlanFl 40X) also played an important role. Precise adjustments of the compensation ring of the objective and the shear amount of the Nomarski prism were indispensable for obtaining a high contrast level of elementary steps.

Preparation of Solutions and Seed Crystals. For in situ observation of elementary steps under high pressure, seed crystals were placed directly on the sapphire window of the high-pressure vessel to minimize the optical aberration. The seed crystals were prepared as follows. A suspension of GI crystals (Hampton Research Co., Ltd., HR7-100), containing 0.91 M ammonium sulfate and 1 mM magnesium sulfate in 6 mM tris hydrochloride buffer (pH = 7.0) (Tris-HCl is known as the most insensitive buffer to pressure[22]), was dissolved (~33 mg mL^{-1}) and filtered as described in ref 3. Then

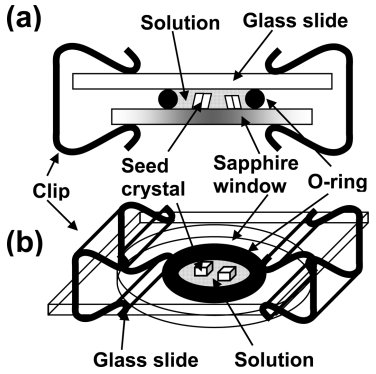

Figure 2. Schematic illustration of a setup for the preparation of seed crystals: a side view (a) and a bird's-eye view (b).

the filtrate was transferred onto the sapphire window and sealed with an O-ring and a glass slide as shown schematically in Figure 2.

After a few small crystals appeared on the window at 10 °C, the crystals were grown at room temperature (~ 22 °C) until they reached an appropriate size for the observation (typically ≥100 μm). The crystals placed on the window were rinsed with a GI solution of 5.6 mg mL^{-1}, and then the window with the crystals was fitted into the high-pressure vessel filled with a GI solution of 5.6 mg mL^{-1}. In this study, we prepared ≤10 crystals (size ~ 150 μm) in the 1.6 mmϕ O-ring on the sapphire window. Thus, the average separation between the crystals was ~300 μm.

Results and Discussion

Direct Observation of Elementary Steps under High Pressure. We attempted to visualize individual elementary steps of GI crystals at 50 MPa. Figure 3 shows photomicrographs of a {011} face of a GI crystal at 50 MPa (a−c) and 0.1 MPa (d). Figure 3a−c presents the time course of the growth of 2D islands. The 2D islands spread with growth time. When the steps of neighboring 2D islands coalesced, the contrast of the steps disappeared completely, as in the regions indicated by black arrows in (b) and (c). As shown in Figure 3a−c, we observed 71 detectable collisions in total and the contrast among all steps disappeared in this way.

Here, it is important to prove whether the steps we observed were elementary ones or not. To discuss this issue quantitatively, first we assume that we cannot visualize any step whose height is below a critical height h_c. In such a case, when a detectable step (whose height $h \geq h_C$) and an undetectable step (whose height $h' < h_C$) collide and the height difference $\Delta h \equiv |h - h'|$ is less than h_C, the detectable step apparently disappears after the coalescence. However, we did not observe such a sudden apparent disappearance of step in this study, although it should occur frequently if the steps that we observed were not elementary ones.

For simplicity, we assume that there are only two types of steps; an elementary step E and a double-layered step D. We define x ($0 \leq x \leq 1$) as a fraction of E steps: the fraction of D steps equals $(1 - x)$. When we cannot observe the E steps but can observe the D steps ($h_e < h_C \leq 2h_e$, h_e: the height of the E step), the probability of the apparent disappearance (P_{dis}) of the D steps caused by the collision with the E steps is expressed as,

$$P_{dis} = 2x(1-x) \quad (1)$$

As shown in Figure 3, we observed the coalescences of 2D islands, that is, visible D steps. The probability of such coalescences P_{coal} is expressed as

$$P_{coal} = (1-x)^2 \quad (2)$$

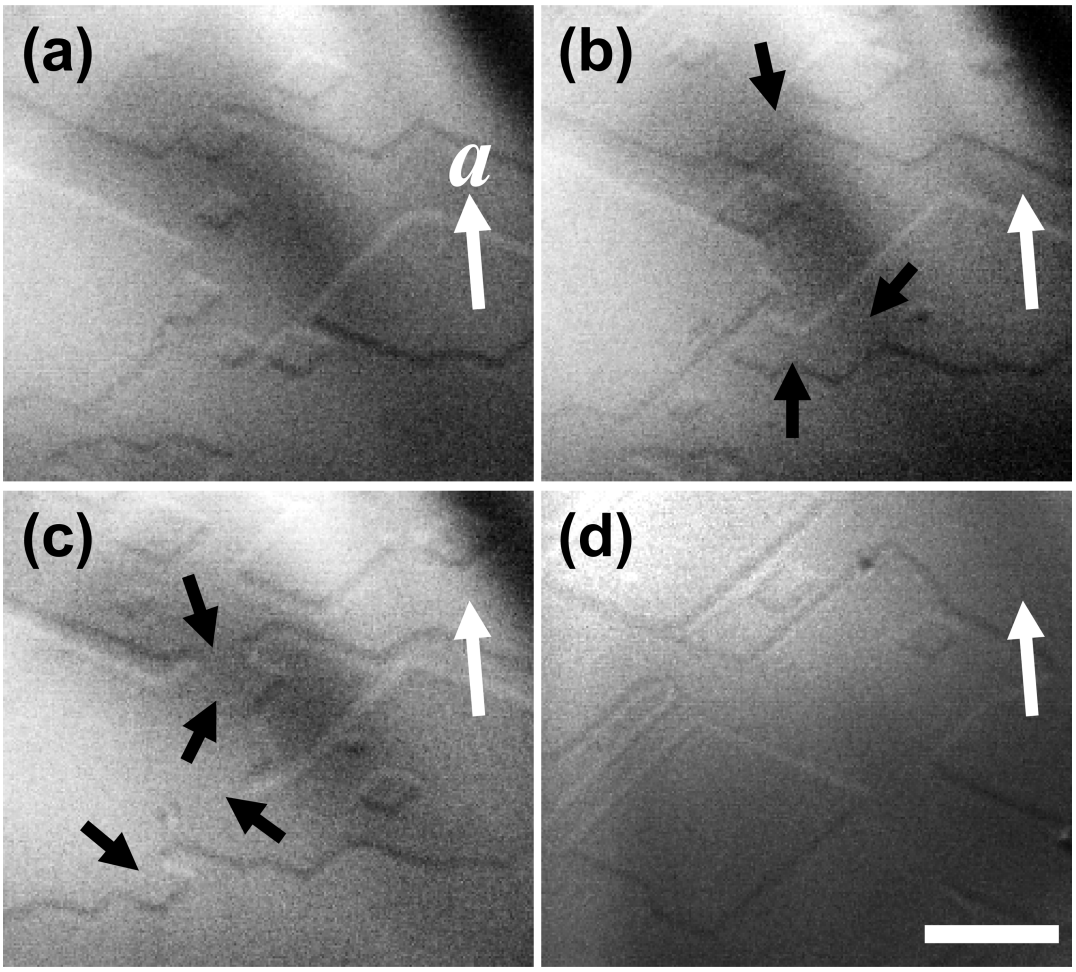

Figure 3. Surface microtopographs of a {011} face of a GI crystal at 50 MPa (a−c) and 0.1 MPa (d). The sequences of micrographs show the time course of 2D nucleation growth of the polynucleation type: 0 s (a), 240 s (b), and 480 s (c). Black arrows in (b) and (c) show the regions at which the contrast between the coalesced steps disappeared. The same crystal in the same solution was observed at both pressures by LCM-DIM. White arrows indicate the ⟨100⟩ directions of the crystal. The scale bar represents 10 μm. GI concentration: 5.6 mg mL^{-1} at 26.4 °C.

Since we did not observe the apparent disappearance during 71 detectable coalescences, the ratio of P_{dis} to P_{coal} should be smaller than 1/71:

$$P_{dis}/P_{coal} = 2x/(1-x) < 1/71 \quad (3)$$

The solution of the inequation 3 with respect to x is $x < 1/143$. In this case, almost all steps present on crystal surfaces are the D steps, and a very small fraction of E steps exists. However, it is obviously an unnatural case, since in such a case the D steps should be redefined as the elementary ones. In the future, this picture will be statistically proven with an increasing number of collision observations. In the case of steps higher than two layers, the solutions to the inequation $P_{dis}/P_{coal} < 1/71$ become more unnatural, as explained in Supporting Information. Therefore, we conclude that elementary steps present in ample quantity can be visualized by LCM-DIM under high pressure.

In addition, from AFM observations of GI crystal surfaces, the typical step height was estimated to be 7.0 ± 0.7 nm. This value is very consistent with the height of elementary steps on the {011} face (7.2 nm) calculated from crystallographic data.[23] In the case of tetragonal lysozyme crystals, we succeeded in observing shorter elementary steps (5.6 and 3.4 nm on {110} and {101} faces, respectively) by LCM-DIM.[6] Therefore, it is also reasonable to conclude in this study that we observed elementary growth steps of 7.2 nm in height. We emphasize that, for the first time to our knowledge, we succeeded in directly observing individual elementary steps under high pressure, by utilizing LCM-DIM and the high-pressure vessel designed specially in this study.

In our previous study,[4] we reported the kinetic acceleration of the growth of {101} faces by pressure. A GI crystal is bounded by three kinds of faces: {101}, {011}, and {110}. Hence, to clarify the entire picture of kinetic acceleration by pressure, we observed {011} faces in this study. In Figure 3, rhombus-shaped 2D islands, similar to those observed previously on a {101} face at 0.1 MPa,[4] were also formed on a {011} face at 0.1 and 50 MPa. The shape and orientation of the islands on a {011} face were not changed, irrespective of pressure. This result suggests that our hypothesis in the previous study[4] was probably correct: irrespective of pressure, {101} faces of GI crystals grow by 2D nucleation growth of the polynucleation type as {011} faces do. In the near future, we will report the in situ observation of all three kinds of surfaces under high pressure.

Solubility Curve Determination by in Situ Observation of Steps and Ridges. We next determined equilibrium temperatures of GI crystals T_e in solutions of given GI concentrations

by in situ observation of steps of 2D islands and ridges of crystals under high pressure. If the temperature of the sample is set below T_e, the steps begin to advance as shown in Figure 3a−c (supersaturated). On the other hand, if the temperature is raised higher than T_e, steps of 2D islands and ridges of crystals start to dissolve (undersaturated). Figure 4 shows typical examples of the growth and dissolution of GI crystal ridges under high pressure (25 MPa). In Figure 4a, white arrows show the pits on ridges prepared by previous dissolution of the crystal. During the growth at 32.5 °C, the dissolution pits shown in Figure 4a disappeared, as shown in Figure 4b. In contrast, the dissolution pit that was not fully repaired during the growth (Figure 4b: black arrow) was enlarged during the subsequent dissolution at 34.3 °C (Figure 4c). The maximum temperature at which the growth of crystals was observed corresponds to the minimum temperature of equilibrium (T_{min}), and the minimum temperature at which dissolution was detected shows the maximum temperature of equilibrium (T_{max}). Hence, from T_{max} and T_{min} measured experimentally, we determined the equilibrium temperature (T_e) and its error (δT_e) as $T_e = (T_{max} + T_{min})/2$ and $\delta T_e = (T_{max} - T_{min})/2$, respectively.

Strictly speaking, we cannot determine true equilibrium conditions using a crystal that has a growth shape. However, in the case of protein crystals, such ideal determination of true equilibrium conditions is almost impossible; since protein crystals grow very slowly, a period longer than a couple of months is necessary,[10,24,25] and during such a long period a protein solution is easily deteriorated.[26] Hence, most of the previous solubility measurements of protein crystals were based on the determination of conditions of zero growth or dissolution using crystals with growth shapes, at the expense of strictness.

Figure 5a shows the solubility curves thus determined at 0.1, 25, and 50 MPa (open symbols): one equilibrium temperature was determined within ~1 h. The solubility curve determined by TBI at 0.1 MPa (solid symbols) in the previous study[3] is also plotted. Although our data are still preliminary at present, a C_e vs T_e plot shifts toward a higher temperature region with increasing pressure. Thus, the solubility C_e of GI crystals decreases significantly with increasing pressure, as reported previously,[3] indicating that the driving force for crystallization increases significantly with increasing pressure.

In addition, we noticed a significant difference in the amounts of δT_e determined by both methods. In particular, under a low concentration range, δT_e of open circles becomes much smaller than those of solid circles, as shown in Figure 5b. This result indicates that the solubility curve determination by the observation of individual steps and ridges is much more sensitive than that by TBI via concentration distributions around growing or dissolving crystals. The poorer precision of TBI compared to LCM-DIM is due to the greater consumption of solute molecules necessary to detect the growth or dissolution of a crystal. In the case of a lysozyme crystal, about five layers of elementary steps should sweep a whole crystal surface for shifting interference fringes by 1/10 of a fringe interval, which is the typical minimum fringe shift necessary for detection.[10] In contrast, LCM-DIM requires only a slight change in the position of steps or the shape of ridges to detect the growth or dissolution of a crystal.

Furthermore, the solubility curve at 0.1 MPa determined by the observation of steps and ridges is shifted toward a higher temperature direction (Figure 5a), and is located

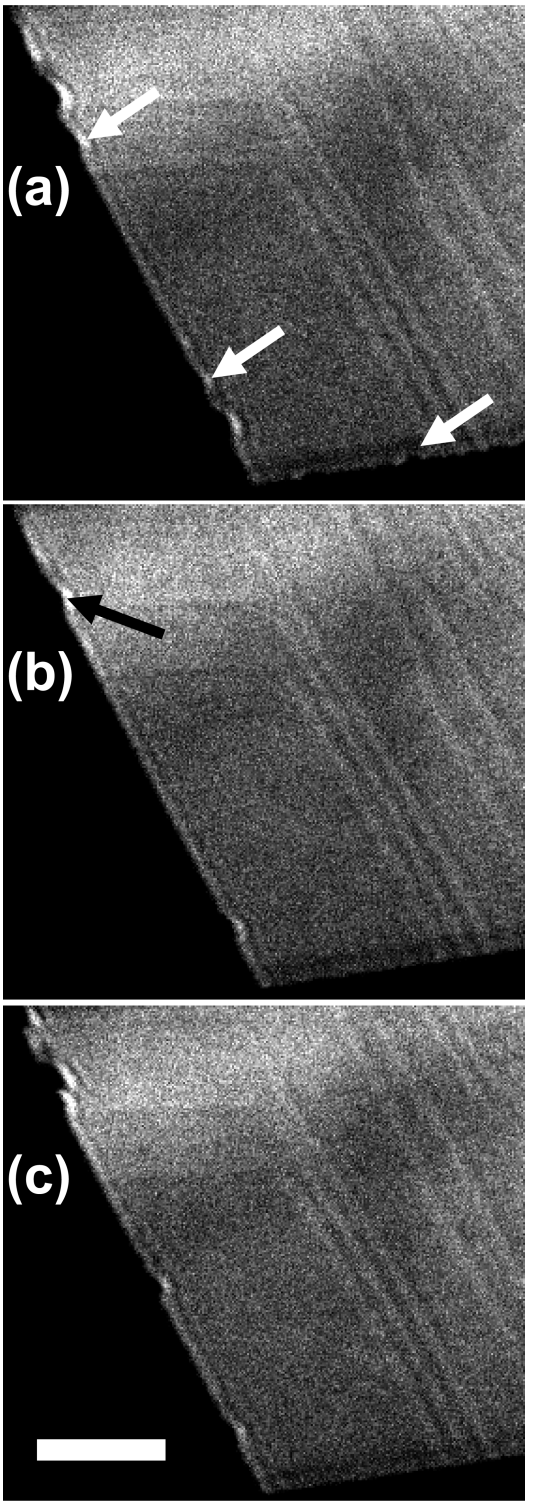

Figure 4. Growth and dissolution of a GI crystal ridge at 25 MPa. (a) 0 s: start at 32.7 °C, (b) 780 s: growth at 32.5 °C, (c) 2130 s: dissolution at 34.3 °C. White arrows in (a) show pits prepared by previous dissolution. The pits disappeared in (b) because the growth occurred during 780 s. The pit indicated by the black arrow in (b) shows the points from where the dissolution starts. Scale bar represents 10 μm.

around the border of δT_e determined by TBI. This result shows that the T_e measurement by TBI is insensitive particularly to growth because the rate of growth is slower than that of dissolution, in addition to the indirectness of the method. It should also be emphasized that δT_e by step

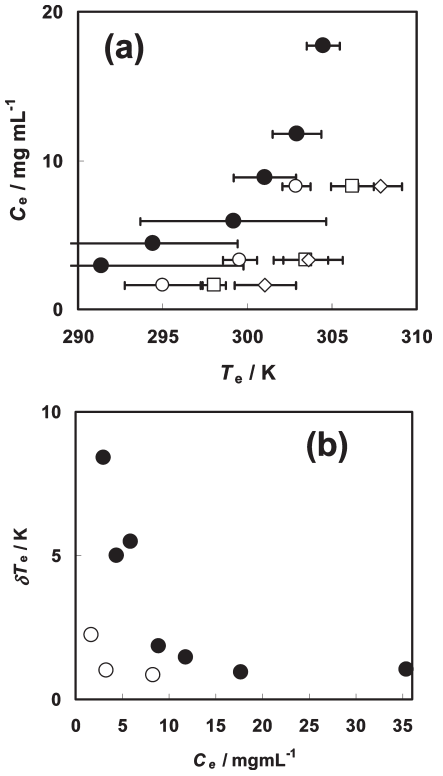

Figure 5. Solubility curve determination. (a) Changes in solubilities C_e of GI crystals as a function of equilibrium temperature T_e, determined by the in situ observation of steps and ridges at 0.1 MPa (○), 25 MPa (□) and 50 MPa (◇). A solubility curve determined by two-beam interferometry at 0.1 MPa (●)[3] is also plotted in the figure. Error bars show the accuracy of equilibrium temperature determination. (b) Changes in errors of equilibrium temperatures δT_e as a function of solubility C_e: the error determined by the in situ observation of steps and ridges at 0.1 MPa (○) and those determined by two-beam interferometry at 0.1 MPa (●).

observation can be decreased with a longer observation period, although δT_e by TBI does not depend on the time period once the concentration distribution around a crystal reaches a steady state. Although this study's error bars at the higher temperature side deviated slightly from those by the TBI methods, we could not offer any theoretical explanation other than the use of a different lot of GI sample.

2D Nucleation Rate and Step Velocity under High Pressure. We also measured in situ 2D nucleation rates J_s (Figure 6a) and step velocities V (Figure 6c) of 2D islands on the {011} face at 0.1, 25, and 50 MPa. Figure 6b shows the step advance L of typical steps with time. The L increases linearly with time: the supersaturation state did not change during the measurements. From these plots, we determine the V. As shown in Figure 6a,c, J_s and V increased with increasing pressure. For these plots, GI concentration in the bulk solution C (= 5.6 mg mL^{-1}) and temperature T (= 26.4 °C) were constant throughout the measurement. Thus, the increases in J_s and V are due completely to the increase in pressure. Further data accumulation will enable us to determine surface free energy, activation energy, or activation volume[27] from the dependence of J_s or V on temperature or pressure.

Here it should be important to check whether the results shown in Figure 6 are valid or not, that is, whether solute concentration at a crystal surface was the same as that of a bulk solution. We then discuss the rate-determining step of

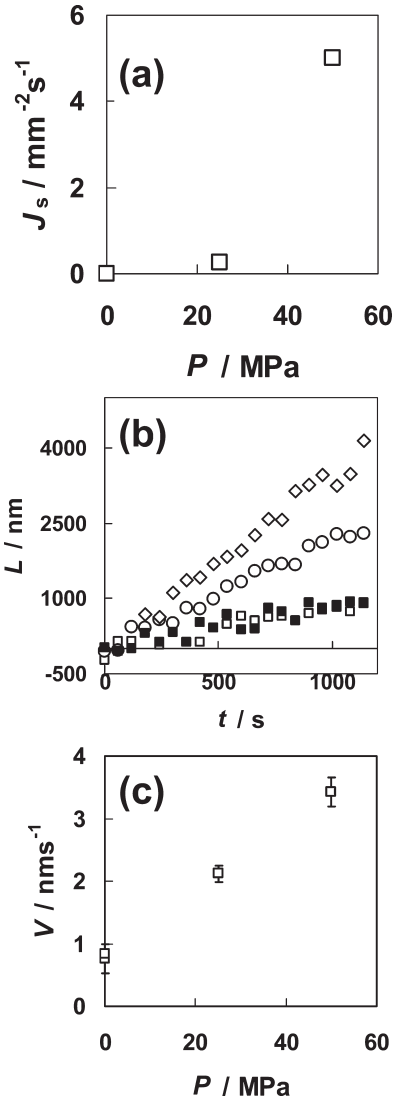

Figure 6. 2D nucleation rates J_s with pressure (a) of 2D islands on the {011} faces of GI crystals, advancement of typical steps L with time (b), and step velocities V with pressure (c). In (b), L was measured at 0.1 MPa (■ and □), 25 MPa (○), and 50 MPa (◇). GI concentration in a bulk solution is 5.6 mg mL^{-1} and temperature is 26.4 °C. Error bars of V in (c) are the standard deviations of V of five different islands.

the growth of GI crystals. Crystal growth is governed by the surface reaction or the bulk diffusion process. It is known that a dimensionless number K can be a good measure for this evaluation,[28]

$$K = \beta_f \frac{\delta}{D} \tag{4}$$

Here, β_f is the face kinetic coefficient, D is the bulk diffusivity of solute, and δ is the characteristic diffusion length (the thickness of a solute depletion zone). In the case of lysozyme crystals, Vekilov and Rosenberger obtained $K = 0.05$ using $\beta_f = 10^{-8}$ m s^{-1}, $D = 7 \times 10^{-11}$ m^2 s^{-1}, and $\delta \approx 3 \times 10^{-4}$ m.[8,29,30] Therefore, the bulk diffusion process (D/δ) is much faster than the surface incorporation process (β_f), and the latter becomes the late determining process.

In the case of GI crystals, the molecular weight 173 kDa is about 10 times that of lysozyme (14.3 kDa). Hence, the bulk diffusivity of GI becomes $10^{1/3}$ times smaller than that of lysozyme (D of GI = 3×10^{-11} m^2 s^{-1}). In contrast, the

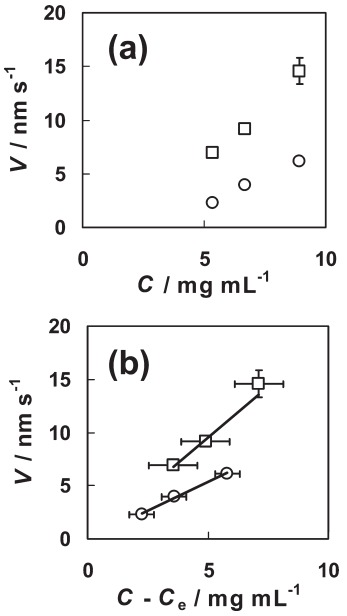

Figure 7. Step velocities V on the {011} faces of GI crystals as a function of C (a) and $C - C_e$ (b). V was measured at 0.1 MPa (○) and 50 MPa (□). Temperature was 25.0 °C. The lines shown in (b) indicate the results of weighed linear fitting.

values of β_f evaluated from our previous data[4] were $\beta_f = 1 \times 10^{-10}$ m s^{-1} at 0.1 MPa and $\beta_f = 6 \times 10^{-10}$ m s^{-1} at 100 MPa: β_f of GI is 1−2 orders of magnitude smaller than that of lysozyme. Since the size of the depletion zone of GI crystals was about $\delta \approx 2 \times 10^{-4}$m,[3] the dimensionless number K of GI is 1 order of magnitude smaller: $K = 7 \times 10^{-4}$ at 0.1 MPa and $K = 4 \times 10^{-3}$ at 100 MPa. These results clearly demonstrate that the growth of GI crystals is much more strongly dominated by the surface reaction process than in the case of tetragonal lysozyme crystals. Hence, we can assume that a surface concentration C_{surf} is almost the same as a bulk concentration C: we can discuss the growth kinetics using the bulk concentration C instead of C_{surf}. As a consequence, the solute depletion zone did not contribute significantly to the growth of the GI crystals.

In addition, we confirmed that the solute concentration in a bulk solution did not change with increasing time during the experiments. Figure 6b clearly indicates that the step velocity (slopes of the plots) and hence the bulk concentration remained constant during the experiments. Step velocities shown in Figure 6c were measured first at 0.1 MPa, then at 25 MPa, 50 MPa, and finally 0.1 MPa again. The final velocity of 0.1 MPa was almost the same as that of the first one, also demonstrating the constant supersaturation in a bulk solution during the measurements (∼90 min).

Step Kinetic Coefficients under High Pressure. Step velocities V on the {011} faces at 0.1 and 50 MPa were measured in the range of protein concentrations C = 5.3 − 8.9 mg mL^{-1}. As shown in Figure 7a, V increased with increasing pressure. The increase in V is attributed to both kinetic and thermodynamic contributions as,[31]

$$V = \beta_{st}\Omega(C - C_e) \quad (5)$$

where β_{st} is the kinetic coefficient of a step, and Ω is the molecular volume of a GI crystal (a GI molecule consists of four identical subunits, and its molar weight is 173 000 g mol^{-1}).[23] We used bulk concentration C instead of C_{surf} as discussed above.

To separate the kinetic contribution (β_{st}) from the thermodynamic one ($C - C_e$), we replotted V as a function of $C - C_e$ (Figure 7b). The solubilities at 25 °C at 0.1 and 50 MPa were 3.1 ± 0.5 and 1.8 ± 1.0 mg mL^{-1}, respectively (errors of solubilities were estimated from the errors in Figure 5). The slopes of the straight lines shown in Figure 7b correspond to $\beta_{st}\Omega$ in eq 5 at 0.1 and 50 MPa. We have measured Ω under 100 MPa by X-ray crystallography, and found that Ω decreased by only 1.1% with increasing pressure: Ω were $(4.79 \pm 0.03) \times 10^{-25}$ and $(4.74 \pm 0.08) \times 10^{-25}$ m^3 at 0.1 and 100 MPa, respectively.[32] Thus, we concluded that β_{st} increased with increasing pressure kinetically. β_{st} values thus obtained were $(6.4 \pm 0.4) \times 10^{-7}$ and $(11.4 \pm 1.7) \times 10^{-7}$ m s^{-1} at 0.1 and 50 MPa (here we assume that Ω at 50 MPa is same as that at 0.1 MPa), respectively. Further data accumulation will enable us to determine activation energy for a solute molecule to be incorporated into a kink site ε_{kink} and activation volume $\Delta V^{\ddagger}$[27] from the dependence of β_{st} on temperature and pressure, respectively.

Conclusions

In this study, we have, for the first time, attempted to observe in situ the elementary steps on the {011} faces of GI crystals under high pressure (up to 50 MPa), utilizing the LCM-DIM system and the specially designed high-pressure vessel with the 1 mm-thick sapphire window. The key findings obtained in this study are as follows:

(1) The elementary steps (7.2 nm high) of the 2D islands were observed in situ under high pressure with a sufficiently high contrast level.
(2) Irrespective of pressure, the {011} faces grew by 2D nucleation growth of the polynucleation type. The growth morphology was not changed by pressure.
(3) The solubility curves determined by the observation of steps and ridges were significantly more precise than those determined by TBI, particularly in the low GI concentration range.
(4) The 2D nucleation rate and step velocity increased with increasing pressure at C = 5.6 mg mL^{-1} and T = 26.4 °C.
(5) Step kinetic coefficient β_{st} on the {011} faces of a GI crystal increased with increasing pressure at 25.0 °C.

Acknowledgment. The authors wish to thank Dr. Masahide Sato of Kanazawa University for valuable discussions on the step−step interaction induced by entropy. This work was supported by Grants-in Aid (Nos. 16760014 and 19760009 (Y.S.), No. 18360003 (G.S.)) of Scientific Research of the Ministry of Education, Culture, Sports, Science and Technology Japan. This work was performed under the interuniversity cooperative research program of the Institute for Materials Research, Tohoku University.

Supporting Information Available: Precise explanations on the solutions to the inequation $P_{dis}/P_{coal} < 1/71$ in the case of steps higher than two layers. This material is available free of charge via the Internet at http://pubs.acs.org.

References

(1) http://proteome.bnl.gov.
(2) Visuri, K.; Kaipainen, E.; Kivimaki, J.; Niemi, H.; Leisola, M.; Palosaari, S. *Bio/Technology* **1990**, *8*, 547–549.
(3) Suzuki, Y.; Sazaki, G.; Visuri, K.; Tamura, K.; Nakajima, K.; Yanagiya, S. *Cryst. Growth Des.* **2002**, *2*, 321–324.

(4) Suzuki, Y.; Sazaki, G.; Matsui, T.; Nakajima, K.; Tamura, K. *J. Phys. Chem. B* **2005**, *109*, 3222–3226.
(5) Galkin, Oleg; Vekilov, P. G. *J. Phys. Chem. B* **1999**, *103*, 10965–10971.
(6) Van Driessche, A. E. S.; Sazaki, G.; Otalora, F.; Gonzalez-Rico, F. M.; Dold, P.; Tsukamoto, K.; Nakajima, K. *Cryst. Growth Des.* **2007**, *7*, 1980–1987.
(7) Komatsu, H.; Miyashita, S.; Suzuki, Y. *Jpn. J. Appl. Phys.* **1993**, *32*, L1855–L1857.
(8) Miyashita, S.; Komatsu, H.; Suzuki, Y.; Nakada, T. *J. Cryst. Growth* **1994**, *141*, 419–424.
(9) Kurihara, K.; Miyashita, S.; Sazaki, G.; Nakada, T.; Suzuki, Y.; Komatsu, H. *J. Cryst. Growth* **1996**, *166*, 904–908.
(10) Sazaki, G.; Kurihara, K.; Nakada, T.; Miyashita, S.; Komatsu, H. *J. Cryst. Growth* **1996**, *169*, 355–360.
(11) Suzuki, Y.; Sawada, T.; Miyashita, S.; Komatsu, H. *Rev. Sci. Instrum.* **1998**, *69*, 2720–2724.
(12) Sazaki, G.; Nagatoshi, Y.; Suzuki, Y.; Durbin, S. D.; Miyashita, S.; Nakada, T.; Komatsu, H. *J. Cryst. Growth* **1999**, *196*, 204–209.
(13) Suzuki, Y.; Sawada, T.; Miyashita, S.; Komatsu, H.; Sazaki, G.; Nakada, T. *J. Cryst. Growth* **2000**, *209*, 1018–1022.
(14) Markov, I. V. In *Crystal Growth for Beginners*; World Scientific: Singapore, 1995; Chapter 3, p 196.
(15) Durbin, S. D.; Carlson, W. E. *J. Cryst. Growth* **1992**, *122*, 71–78.
(16) Durbin, S. D.; Carlson, W. E.; Saros, M. T. *J. Phys. D* **1993**, *26*, B128–B132.
(17) McPherson, A.; Malkin, A. J.; Kuznetsov, Y. G. *Annu. Rev. Biophys. Biomol. Struct.* **2000**, *29*, 361–410.
(18) Higgins, S. R.; Eggleston, C. M.; Knauss, K. G.; Boro, C. O. *Rev. Sci. Instrum.* **1998**, *69*, 2994–2998.
(19) Sazaki, G.; Matsui, T.; Tsukamoto, K.; Usami, N.; Ujihara, T.; Fujiwara, K.; Nakajima, K. *J. Cryst. Growth* **2004**, *262*, 536–542.
(20) Sazaki, G.; Tsukamoto, K.; Yai, S.; Okada, M.; Nakajima, K. *Cryst. Growth Des.* **2005**, *5*, 1729–1735.
(21) Abe, J.; Hirano, N.; Tsuchiya, N. *Jap. Mag. Mineral. Petrol. Sci.* (*in Japanese*) **2006**, *35*, 187–196.
(22) Neuman, R. C., Jr.; Kauzmann, W.; Zipp, A. *J. Phys. Chem.* **1973**, *77*, 2687–2691.
(23) Carrell, H. L.; Glusker, J. P.; Burger, V.; Manfre, F.; Tritsch, D.; Biellmann, J. −F. *Proc. Natl. Acad. Sci. U. S. A.* **1989**, *86*, 4440–4444.
(24) Rosenberger, F.; Howard, S. B.; Sowers, J. W.; Nyce, T. A. *J. Cryst. Growth* **1993**, *129*, 1–12.
(25) Pusey, M. L.; Gernert, K. *J. Cryst. Growth* **1988**, *88*, 419–424.
(26) McPherson, A. In *Crystallization of Biological Macromolecules*; Cold Spring Harbor Laboratory Press: New York; Chapter 8, pp 338−345.
(27) Laidler, K. J. In *Chemical Kinetics*, 3rd ed.; Harper & Row: New York, 1987; pp 206−209.
(28) Vekilov, P. G.; Rosenberger, F. *Phys. Rev. Lett.* **1998**, *80*, 2654–2656.
(29) Komatsu, H.; Miyashita, S.; Suzuki, Y. *Jpn. J. Appl. Phys.* **1993**, *32*, L1855–L1857.
(30) Lin, H.; Rosenberger, F.; Alexander, J. I. D.; Nadarajah, A. *J. Cryst. Growth* **1995**, *151*, 153–162.
(31) Chernov, A. A. In *Modern Crystallography III*; Springer −Verlag: Berlin Heidelberg New York Tokyo, 1984; p 108.
(32) Tsukamoto, M. Master Thesis, Graduate School of Advanced Technology and Science, The University of Tokushima, March **2009**.